An alternative route to nanoscale aggregates with a pH-responsive random copolymer copolymer

Jonathan C. Pegg,[†] Adam Czajka,[†] Christopher Hill,[†] Craig James,[†,¶] Jocelyn Peach,[†] Sarah E. Rogers,[‡] and Julian Eastoe[*,†]

[†]*School of Chemistry, University of Bristol, Cantock's close, Bristol, , BS8 1TS, UK*

[‡]*ISIS-STFC, Rutherford Appleton Laboratory, Chilton, Oxon OX11 0QX, UK*

[¶]*Current address: Department of Chemistry and CSGI, University of Florence, 50019 Sesto Fiorentino, Firenze, Italy*

E-mail: julian.eastoe@bristol.ac.uk

Phone: +44 (0) 117 928 9180

Abstract

A random copolymer, poly(methyl methacrylate-co-2-dimethylaminoethyl methacrylate) (poly(MMA-co-DMAEMA)) is shown to form nano-scale aggregates (NAs) ($\sim$ 20 nm) at copolymer concentrations $\geq$10 % w/w, directly from the pre-formed surfactant-stabilised latex ($\sim$ 120 nm) in aqueous solution. The copolymer is prepared by a conventional emulsion polymerisation. Introducing a small mole fraction of DMAEMA ($\sim$ 10 %) allows the copolymer hydrophilicity to be adjusted by pH and external temperature, generating NAs with tuneable sizes and defined weight-average aggregation number, as observed by dynamic-light scattering (DLS) and small-angle neutron scattering (SANS). These NAs are different to the so-called mesoglobular systems, and are

insensitive to temperature at fixed pH. The relatively broad chemical composition distribution of the copolymer and 'lumpy' (or 'blocky' but not diblock) incorporation of DMAEMA, means that the NAs cannot be simply thought of as conventional polymer micelles. In the acidic pH regime the amphiphilic copolymer exhibits a defined critical aggregation concentration (CAC) and a minimum air-water surface tension of 45.2 mN m^{-1}. This copolymer represents a convenient route to self-assembled NAs, which form directly in aqueous dispersions after pH- and temperature-triggers, rather than the typically applied (and time-consuming) water-induced micellisation approach. compound micelles

Introduction

Intermolecular aggregation is an important consequence of amphiphilic character in polymers and surfactants.[1] Common A-B block copolymers (fig. 1), comprised of monomer pairs A and B with appreciably different solubilities, can self-assemble into nanoscale aggregates (or micelles) and find a range of applications in photoelectrics, micro-electronics and perhaps most significantly in the biomedical fields.[2–6] For these systems an intriguing question comes to mind: "is it really necessary to use true A-B block copolymers for stabilising interfaces and micellar-like aggregates?" In (perfectly) random copolymers (fig. 1) the probability of finding a given monomer at any point along the polymer chain is given by its respective mole fraction. In reality, the chemical nature of the monomers and the copolymerisation strategy (solubility of monomers,[7,8] monomer reactivity ratios,[9,10] or feed strategies[11]) mean that that the copolymer microstructure can deviate from being statistically random to even quite 'lumpy' (or 'blocky').

Advances in controlled polymerisation techniques,[12–15] have allowed for the synthesis of well-defined block architectures, with dispersity ($Đ = M_w/M_n$) approaching 1.0. Courtesey of their structural regularity and compositional tuneability, block copolymers exhibit predictable and controllable self-assembly properties.[16,17] However, the synthetic routes to these

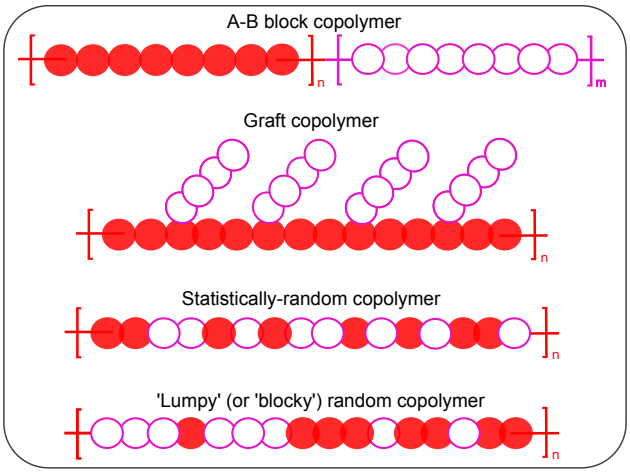

Figure 1: ..."is it really necessary to use true A-B block copolymers for stabilising interfaces and micellar-like aggregates?" Copolymers can be broadly categorised as either block, graft or random type, according to the arrangement of monomers in the polymer backbone. In block copolymers, the monomers are distributed as clearly segregated sections of each monomer. In (perfectly) random copolymers, the monomers are arranged so that the probability of finding a given monomer at any point along the polymer chain is given by its respective mole fraction. 'Lumpy' (or 'blocky') random copolymers have a microstructure intermediate between block and (perfectly) random, so that the copolymers have a more lumpy monomer distribution.

polymers can require costly precursors, and are tedious and time-consuming, involving sequential controlled polymerisation or post polymerisation steps. On the other hand, random copolymers are much easier to prepare and can be accessed from more conventional free radical polymerisation routes; in some instances these more primitive polymers have been shown to self-assemble, despite their less well-defined structures.[18–28] Hence, random copolymers are much more amenable for industrial and commercial applications. For this class of random copolymers it becomes of interest to know if lumpy molecular architectures (see fig. 1) are able to adsorb to interfaces and self-assemble, or whether true A-B architectures are needed.

This present work introduces a new random copolymer, poly(methyl methacyrlate-co-2-dimethyl aminoethyl methacylate) (poly(MMA-co-DMAEMA)). The polymer is prepared by a routine aqueous emulsion free-radical polymerisation with only a small molar fraction of DMAEMA ($\sim 10\%$). Poly(DMAEMA) is a polycation that is, along with its copolymers,

well known for pH- and thermoresponsive behaviour, exhibiting an accessible lower critical solution temperature (LCST), making it an important polymer in emerging biomedical[29,30] and materials[31,32] applications. Incorporated in a lumpy fashion, DMAEMA imparts a pH and temperature responsiveness, which allows the hydrophilicity of the polymer to be tuned. The approach taken here is to first form a surfactant-stabilised latex, which then generates self-assembled nano-aggregates (NAs) in aqueous media by pH and temperature triggers. The term NAs has been deliberately chosen to distinguish the systems of interest here against polymer micelles[2,16] (formed from block copolymers) and thermoresponsive mesoglobules (which are globular-phase intermolecular aggregates formed by thermoresponsive polymers and their copolymers, which eventually disassociate at temperatures below their LCST.)[33–35] A further significance of the new copolymer system is the ability to form self-assembled NAs directly in aqueous solution, avoiding the more time-intensive water-induced micellisation (WIM)[16,22] route. In the WIM method, the copolymer is dissolved in a common solvent (for both monomers), followed by the gradual addition of water up until a critical water concentration (CWC), at which point micro-phase separation occurs. Finally, the cosolvent is removed (normally by dialysis against water) to leave the aggregates dispersed in aqueous solution. To reiterate, here self-assembled NAs can be formed directly in aqueous phases. Surface tension measurements show the polymer adsorbs effectively at the air-water interface and small-angle neutron scattering (SANS), together with dynamic-light scattering (DLS) and zeta potential measurements (electrophoresis) have been used to characterise the self-assembly properties and morphology of the nano-aggregates, as a function of pH. Pyrene was used as a fluorescence probe to provide evidence for internal hydrophobic domains in the copolymer aggregates.

Experimental Section

Materials

Methyl methacrylate (MMA) (Aldrich, 99 %) and 2-Dimethylaminoethyl methacrylate (DMAEMA) (Aldrich, 98 %) contained trace amounts of Monomethyl ether hydroquinone (MEHQ) as an inhibitor. MEHQ was removed from monomers immediately prior to use, by passing through a column of Aluminium Oxide (activated, basic, Brockmann 1). 1-Dodecanethiol (Aldrich, $\geq$ 98 %), Ammonium persulfate ($\geq$ 98 %), Pyrene (Acros, puriss $\geq$ 99%), Deuterium Oxide (Aldrich, 99.9 %) and anionic surfactant Rhodafac RS710E (Rhodia, 30% in water) were used as received. Rhodofac RS710E is a widely used dispersant, emulsifier and wetting agent. It is a Polyethoxylene tridecyl phosphate monoester, with 10 EO units and a critical micelle concentration (CMC) of 0.055 % w/w $\equiv$ 0.74 mM (conductivity).

Methods

Synthesis of Poly(MMA-co-DMAEMA) copolymer

Poly(MMA-co-DMAEMA) copolymer was prepared by a free-radical aqueous emulsion polymerisation. A separate 'pre-emulsion' (monomer feed) and initiator feed were prepared and degassed (N_2, 2 hr). The monomer feed was prepared by mixing monomers MMA (22.8 g) and DMAEMA (3.95 g) (= 9:1 molar ratio) with deionized water (10.75 g), Rhodofac RS710E (1.40 g, 15 mM in emulsion feed) and chain-transfer agent, 1-Dodecanethiol (0.34 g). The initiator phase was prepared by dissolving Ammonium persulphate (APS) (0.038 g, 1.54 mM) solution in deionized water (5.13 g). An aqueous phase comprising deionized water (59.0 g) and Rhodofac RS710E (0.13 g, 0.89 mM in aqueous phase) was degassed (N_2, 2 hr)and heated to 80°C in a thermostated oil bath. Under magnetic stirring the pre-emulsion and initiator feeds were added simultaneously to the aqueous phase over a 90 min period. Upon completion of the two feeds, the reaction was left to stir for a further 2 hr. The collected copolymer latex dispersion, had a solids content of 23.5 % w/w and a pH of

7.7.

Characterisation of Poly(MMA-co-DMAEMA)

^{1}H-NMR (400 MHz) spectra were acquired on a Jeol ECS 400. The solid copolymer was dissolved in D-Chloroform at a concentration of $\sim$ 20 mg mL^{-1}.

Gel permeation chromatography (GPC) was performed on a Viscotek RImax chromatograph, equipped with an automatic sampler, pump, injector and inline degasser. The column was maintained at 35°C and consisted of styrene/divinyl benzene gels with pore sizes ranging from 500 - 100,000 Å. THF containing 0.1 % w/w [^{n}Bu$_4$N]Br was used as the eluent at a flow rate of 1.0 mL min^{-1}. Samples were dissolved in the eluent at a concentration of 2 mg mL^{-1}. Before analysis, samples solutions were stirred for 1 hr at room temperature and filtered (polytetrafluoroethylene membrane, 0.45 μm pore size). Calibration was conducted using a series of monodisperse polystyrene standards obtained from Aldrich (UK).

Pyrene was used as a fluorescence probe for determining the Critical Assembly Concentration (CAC) of the copolymer. Fluorescence measurements were carried out in quartz cuvettes at 25°C, on a Cary Eclipse (Varian) fluorescence spectrometer. A fixed concentration of pyrene (1.0 x 10^{-6} M) was added to sample vials from a known volume of stock prepared in acetone. The acetone was allowed to evaporate off in air, before polymer solution was added in the concentration range 0.1 - 50 mg mL^{-1}. Fluorescence emission spectra were collected after excitation at λ=337 nm . A slit width of 5 nm was chosen for excitation and emission.

Equilibrium surface tension measurements were collected using a Krüss K100 tensiometer at 25 °C, using the Wilhelmy plate method. Clean surface tension measurements were obtained against deionized water (Millipore, 18.2 MΩ cm). All reported values are obtained from 10 repeat measurements.

Preparation of self-assembled NAs

For the formation of the self-assembled NAs from the copolymer latex dispersion, pH was adjusted with formic acid (10 % w/w in water) to between 4.5 and 2, and further diluted to 17 % w/w, at room temperature. The dispersion was then heated to 65 °C and stirred for 1 hr, before being returned to room temperature. (N.b it is not necessary to cool the latex dispersion to room temperature prior to reducing pH. NAs can be prepared by reducing pH at elevated temperatures conditions required for the polymerisation.)

Surfactant and other impurities were removed from assembled nanoaggregate dispersions by dialysis. Filled tubing (MWCO= 8000 kDa, BioDesign, USA) was immersed in deionized water, with the pH adjusted to 3.7, to ensure good solubility of the copolymer. Removal of surfactant was monitored by equilibrium surface tension measurements: an air-water surface tension of the retentate $\geq$ 70 mN m^{-1} was achieved after $\sim$ 30 days (fig. S1, supporting information.) Given that the surfacatant is expected to interact with the charged polymer, a trace concentration of residual surfactant (below the detection limit of NMR and GPC) may remain dispersed in the 'clean' polymer dispersion.

Characterisation of self-assembled NAs

Dynamic light scattering (DLS) and Electrophoresis (phase-analysis light scattering) measurements were collected at 25°C on a Malvern Nano ZS (4 mW HeNe laser, 633 nm λ). DLS measurements were performed in triplicate on highly dilute aqueous dispersions (10 mM solution of KNO_3 in deionized water). Prior to measurements, samples were filtered (Whatman, 0.1 μm pore size) to remove dust and particulates. The particle size distribution as described in the text is given by the polydispersity index, PDI = [(width of particle size distribution/mean particle size)^2].

Electrophoretic mobility measurements were carried out using a universal dip cell electrode. The pH of polymer dispersions was adjusted using formic acid or sodium hydroxide. Measurements were performed on highly dilute aqueous dispersions at fixed electrolyte con-

centration (10 mM solution of KNO_3 in deionized water) to ensure that measurements were insensitive to acid/base. A conductivity of 1.4 mS $cm^{-1} \pm 0.1$ was observed for all measurements. Reported values are averages of 5 measurements of at least 50 runs. Electrophoretic mobilities were converted to Zeta potentials using the Henry equation and the Smoluchowski approximation.[36]

SANS measurements were performed on the Sans2D instrument at ISIS Pulsed Neutron Source (Didcot, UK). A simultaenous Q-range of 0.004-0.7 $Å^{-1}$ was acheived using an instrument set-up with the source-sample and sample-detector distance of L_1=L_2=4 m with the 1 m^2 detector offset vertically at 60 mm and 100 mm sideways. Samples were kept in Helma quartz cells with a path length of 2 mm, and measured at 25°C. Unless stated otherwise, samples were measured at 0.5 % w/w in Deuterium Oxide (1.5 mM KNO_3, to screen electrostatic interactions). Raw SANS spectra were corrected for scattering from the solvent and cell using the instrument-specific software, Mantid,[37] and set to an absolute intensity scale (cm^{-1}).[38] Data have been fitted, as described in text and in the supporting information, using SasView small-angle scattering software.[39]

Small-Angle Neutron Scattering (SANS) theory

In a SANS experiment, the intensity (I) of scattered neutrons is measured as a function of momentum transfer (or wave-vector) Q, $= (4\pi/\lambda)\sin\theta$, where λ is the neutron wave length and 2θ is the scattering angle. The normalised intensity per unit volume V of N homogeneous isotropic scatterers of volume V_p and scattering length density ρ_p, dispersed in a solvent of scattering length density ρ_s is

$$I(Q) = \Phi V_p(\rho_p - \rho_s)^2 P(Q) S(Q)$$

where $\Phi = (N/V)V_p$ and is the particle volume fraction, the function P(Q) is the particle form factor and S(Q) is the structure factor, responsible for inter-particle interactions. In addition to size and shape information (contained within the particle form factor, P(Q)),

M_w of aggregates can be approximated. For convenience in fitting P(Q) and for zero-angle calculations of the M_w all measurements were carried out at dilute particle concentrations and with background electrolyte so that S(Q→1).

At Q = 0, ($2\theta = 0°$) P(Q) also tends to 1 so that

$$I(Q=0) = \Phi V_p(\rho_p - \rho_s)^2$$

Obviously the intensity of scattering at zero-angle cannot be measured, but rather is determined by extrapolating to Q → 0, using a Guinier plot, $Ln(I(Q)) = Ln(I(0)) - Q^2(R_g^2/3)$, which also gives the particle radius of gyration, and is valid at low-Q for non-interacting particles. In terms of the concentration of polymer (C), I(Q = 0) can also be written

$$I(Q=0) = \Phi V_p(\rho_p - \rho_s)^2 = \frac{CM_w}{d^2 N_A}(\rho_p - \rho_s)^2$$

N_A is Avagadro's constant, and d is the mass density of the polymer. M_w is the molecular weight of the aggregates, which can be compared to the M_w of the free-polymer from the GPC measurement to give the weight-average aggregation number per aggregate, N_{agg}.

Results and Discussion

Characterisation and synthetic considerations of poly(MMA-co-DMAEMA)

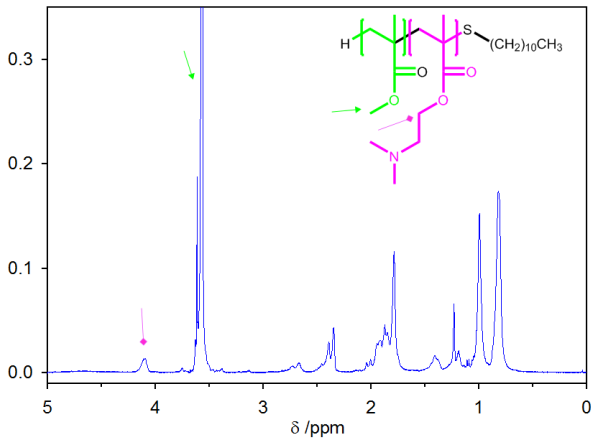

Figure 2: ^{1}H-NMR spectrum of poly(MMA-co-DMAEMA) in D-Chloroform. (Inset) Copolymer molecular structure: repeat units MMA is shwon green and DMAEMA is shown pink. The signals highlighted by the pink (diamond headed) and green arrows correspond to the methylene and methoxy protons from DMAEMA and MMA respectively. The ratio of the these two signals was used to assess the molar ratio of the monomers in the copolymer.

Molecular weight characterisations were carried out by GPC (fig. S2, supporting information); the M_w of the free copolymer was found to be 15.8 kg mol^{-1} with a molecular weight dispersity (Đ= M_w/M_n) = 1.88. The relatively broad Đ is a product of the free-radical emulsion polymerisation. It is important to keep in mind that emulsion polymerisation is a heterogeneous process, with the polymerisation commencing in the aqueous-continuous phase. In emulsion polymerisation the monomer partitions between three phases: the monomer droplets (the monomer reservoir), the aqueous-continuous phase and the surfactant micelle phase (which will become the particle phase, as the polymerisation continues.) As a result of the water-soluble character of the initiator, oligomeric radicals are produced in the aqueous-continuous phase. The final polymer particles formed originate from the primary oligoradicals which enter the micelle (particle) phase, as they become water insoluble with continuing propagation of polymer chains.[40] For this reason, the aqueous phase can play an

important role in governing the microstructure of the polymer latex.[41,42] This is a critical feature of emulsion (co)polymerisation, and is especially pertinent when the two monomers have quite different water-solubilities. DMAEMA (107 g L^{-1} at 25°C) is more water soluble than MMA (15 g L^{-1} at 25°C) and so should be expected to form longer oligomeric chains in the aqueous phase prior to entering the micellar (particle) phase, resulting in the inhomogeneous incorporation of DMAEMA. Some polymer chains will therefore be richer in DMAEMA (and concomitantly more polar),[43] leading to a broadening of the chemical composition distribution (Đ) and resulting in a copolymer with an inherently lumpy microstructure. A lumpy distribution of the more hydrophilic DMAEMA (in the acidic pH regime) might manifest as surface-activity at the air-liquid interface.

The molar ratio of MMA:DMAEMA incorporated in the copolymer is readily calculated from the ratio of the integrals of the signal at $\sim$ 3.6 ppm (from the methoxy group from MMA) and the signal $\sim$ 4.15 ppm (from the methylene on DMAEMA) in the ^{1}H-NMR spectrum (fig. 2). In this way the molar ratio of MMA:DMAEMA in the average copolymer chain = 8.56. The slightly lower incorporation of DMAEMA into the copolymer structure than the monomer ratio in the feed (MMA:DMAEMA = 9.00) was probably due to a small amount of hydrolysis of DMAEMA during the synthesis. Hydrolysis of the ester bond of DMAEMA would result in the incorporation of a trace amount of methacrylic acid (MAA) into the copolymer. Notably, polymers of DMAEMA have been reported to be stable to hydrolysis, even at elevated temperatures.[44,45] With knowledge of the molecular weight and molar compositions of the monomers, it is possible to describe the copolymer by a weight-average degree of polymerisation as follows: Poly(MMA_{134}-co-$DMAEMA_{15}$). Unfortunately, it was not possible to determine the arrangement/sequencing of monomeric units (lumpiness or blockiness) by ^{13}C-NMR, due to the splitting of signals by stereochemical configurations as well as the monomeric sequence, yielding overlapping, complex spectra, precluding quantitative analysis.

It is worth re-emphasising why heterogeneous radical polymerisation routes in aqueous

solution, are industrially attractive, and in many cases are favoured over more controlled polymerisation routes: syntheses are (1) easy to perform and do not require stringent purification, (2) do not require expensive precursors (eg. costly chain-transfer agents) (3) avoid the use of volatile organic compounds and can be performed under mild conditions (4) give access to high molecular weights polymers with higher conversions and faster rates of polymerisation compared to homogeneous polymerisations (bulk or solution).[46] However, their main drawback still remains the unavoidable rapid radical-radical termination reactions, meaning there is a lack of control over Đ and limitations on accessible functionalities and macromolecular architectures.

Route to self-assembled NAs

The tertiary-amino functionality of DMAEMA confers pH- and temperature responsive properties on the copolymer. Therefore, tuning the environmental pH and external temperature provides a convenient means to regulating the polymer solution properties. Reducing pH into the acidic regime and heating triggers dispersion and self-assembly of copolymer chains into NAs with defined weight-average aggregation numbers. The route to self-assembled NAs is represented schematically in fig. 3. For the sake of clarity it is useful to define the aggregation state of the copolymer according to different environmental conditions. Post-polymerisation the copolymer exists as a surfactant-stabilised copolymer latex (i.e domains of copolymer, where the interface with the aqueous phase is stabilised by surfactant,) suspended in aqueous solution, state 'A'. Reducing the pH progressively protonates the phosphate-ester surfactant. In acidic conditions (pH < 5) the surfactant is no longer an effective stabiliser, and the polymer swells into the aqueous phase. At this point the copolymer is a polyelectrolyte, state 'B'. Taking the temperature above ~ 60°C and under constant stirring the copolymer latex particles give way to much smaller intermolecular self-assembled NAs, denoted as the final state 'C'. The particle size distribution (as measured by DLS) of the swollen copolymer latex (state B) and the self-assembled NAs (state C) is given in fig. 4. At this point the NAs

are no longer stabilised by surfactant, but rather by hydrophilic DMAEMA-rich regions at the surface of the aggregates, thereby minimising unfavourable water-interactions with the hydrophobic MMA-predominant cores. The sharp transition in size from B to C is therefore consistent with a transition from a swollen latex (who's size is mostly related to parameters controlled in the synthesis) to intermolecular (nano)aggregates. The actual size transition in itself is fairly immaterial. The DMAEMA-rich stabilising region is made possible by the lumpy structure of the copolymer and can be loosely termed as a corona, with the caveat that the copolymer is a blocky random copolymer, with broad Đ and heterogeneous incorporation of DMAEMA throughout different polymer chains.

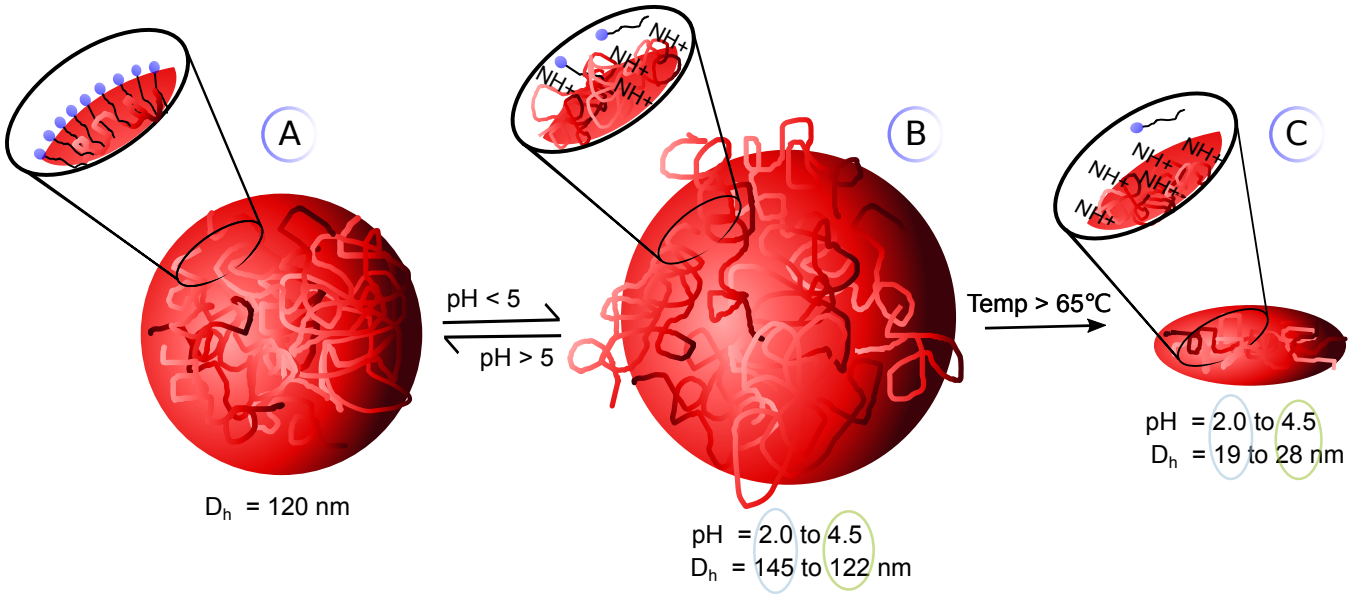

Figure 3: Schematic representation of the route to self-assembled nano-aggregates. (A) Surfactant-stabilised copolymer latex, suspended in aqueous solution, formed by aqueous free-radical copolymerisation. (B) When pH is reduced below 5, the copolymer swells into the aqueous phase. (C) Self-assembled NAs form as the temperature is taken above ~ 60°C with stirring. The size of NAs is a function of the pH, D_h is the hydrodynamic diameter as measured by DLS.

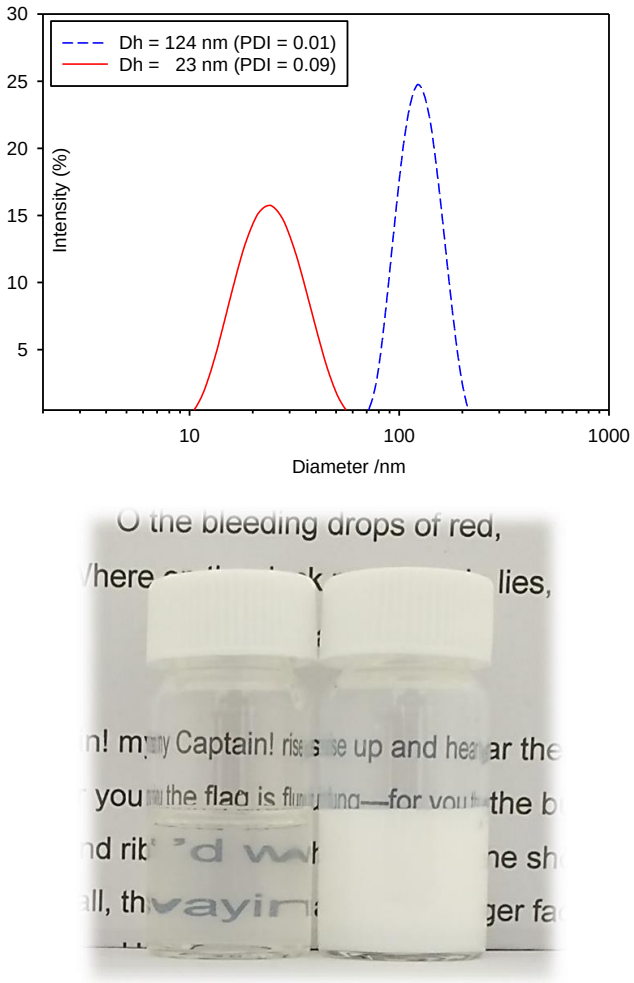

Figure 4: (Upper) the intensity-weighted particle size distribution of the copolymer latex (blue-dashed trace) and self-assembled aggregates (red trace), both at pH 3.5. (Lower) Corresponding visual appearance of dispersions at 17 % w/w. (Right) swollen surfactant-stabilised copolymer latex (state B) strongly scatters light. (Left) Self-assembled nano-aggregates (state C) dispersion weakly scatters light.

The transition from state B to C is accompanied by an increase in viscosity, prior to the formation of smaller self-assembled NAs. Poly(DMAEMA) (and its copolymers) is a well known thermoresponsive polymer.[29,30,47] Under basic conditions, poly(DMAEMA) exhibits an inverse temperature solubility. i.e. a lower critical solution temperature (LCST) at 30-50°C.[47] The LCST is strongly dependent upon pH (charge fraction) and ionic strength.[48] In acidic conditions the hydrophobic collapse (globular-phase) of polymer chains, associated with the LCST, is inhibited by like-charge repulsion and strong enthalpic interactions

with water; remembering the LCST is thermodynamically driven by a unfavourable entropy of mixing, at the expense of enthalpic interactions.[49] Nevertheless, increasing temperature will dehydrate the copolymer and disrupt the balance between inter/intramolecular solvent-polymer, facilitating weak physical association of the polymer at high concentrations ($\geq$12% w/w). With continued stirring (shear) the polyelectrolyte is dispersed and rearranges into NAs, C. The transition from B to C is irreversible, i.e. the surfactant stabilised copolymer latex (A) cannot be recovered from the NAs. Increasing the pH $>$ 5 when the copolymer is in state C leads to either a self-supporting gel at high polymer concentrations ($\geq$5% w/w) or a sedimented layer at lower polymer concentrations.

pH tuneable self-assembly

A threshold pH of at least 4.5, a minimum temperature of $\sim$ 58°C, and a polymer solid concentration of $\geq$12% w/w is needed to bring about an increase in latex dispersion viscosity and the concomitant particle size transition to yield smaller NAs. DLS was used to map the size transitions of the copoymer as a function of pH. (fig. 5.) Reducing pH at room temperature, causes the copolymer latex to steadily swell in the aqueous phase, presumably as DMAEMA groups are increasingly exposed to the aqueous phase and protonated. At pH = 5 the hydrodynamic diameter, D_h = 122 nm, swelling to D_h = 144 nm at pH 2.5. Elevating temperature (before allowing to cool to room temperature) and reducing pH from 4.5 to 2.5 leads to a contraction in D_h, from 28.6 nm to 19.4 nm (see fig. 3). All particle size distributions are monomodal, with low values of the PDI ($\leq$ 0.01 for the surfactant stabilised latex and $\leq$ 0.135 for NAs). Data are tabulated in table S1, supporting information.

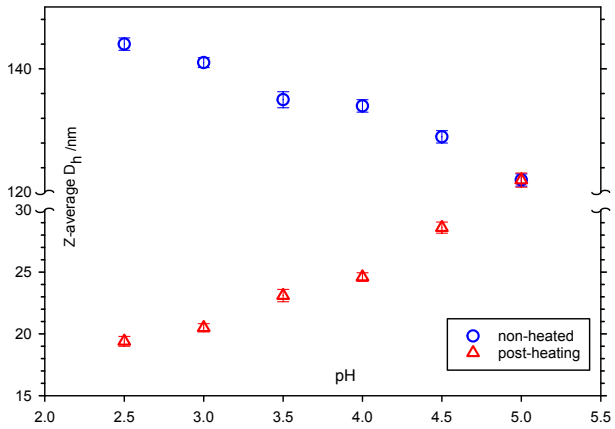

Figure 5: Z-average hydrodynamic diameter (D_h) as a function of pH, for unheated copolymer latex (blue hollow circles) and post-heated assembled-copolymer (red hollow triangles). A critical pH of < 5 is required to form self-assembled nano-aggregates, upon heating to at least 58°C. Error bars are the standard deviations of all data collected, from a minimum of three replicates.

On first consideration this pH-response of the copolymer latex appears curious. Poly(DMAEMA) is a weak polybase, with a system dependent pK_a, normally reported around 7.[50,51] Although, this can vary with ionic strength and with copolymerisation of a hydrophobic monomers. Cotanda et al. showed that the pK_a of poly(DMAEMA-co-MMA) actually increased with higher incorporation of the hydrophobic monomer in the copolymer.[47] This was ascribed to a larger distance between DMAEMA units, in a highly random polymer, facilitating protonation of adjacent amino groups. In the copolymer studied here, the heterogeneous polymerisation results in a lumpy incorporation of DMAEMA monomers. So the proximity of DMAEMA units might make the subsequent protonation of local amine groups more difficult, due to steric hindrance of consecutive protonated units, ultimately decreasing the basicity of the copolymer. Incorporation of a trace amount of MAA into the copolymer, at the expense of DMAEMA, (due to hydrolysis) could also shift the pK_a to slightly lower values. (But there is probably too little acrylic acid to make a conceivable difference to the pK_a.)

In fact, more pertinent is that the DMAEMA groups might be buried in the interior of the copolymer latex at neutral pH. Here, the role of the surfactant stabilising the latex

should not be underplayed. As pH is further reduced an increasing fraction of surfactant is protonated and is no longer effectively stabilising the latex-aqueous phase interface (fig. S3, supporting information). Now, the copolymer is increasingly exposed to the aqueous phase, rendering amino groups available for protonation, and the copolymer swells further into the aqueous phase. Reducing pH further may bring more amino groups to the surface, perpetuating the further swelling of the copolymer into the aqueous phase. So the degree of protonation of the copolymer seems to be inextricably coupled to the pH-behaviour of the residual surfactant. Therefore, the pK_a of DMAEMA, in the normal sense (behaving as a polymer brush in a polymer micelle,[51] for instance) is of less significance in understanding the pH-response of this synergistic copolymer/surfactant system.

pH/temperature-response of NAs

Interestingly, it was found that the self-assembled NAs also exhibit responses to pH and temperature. This provides an opportunity to study the correlation between NA surface charge (Zeta potential, ζ) and size (hydrodynamic diameter). Heating the copolymer latex at pH 3.5 gives NAs with $D_h = 23.3 \pm 0.3$ nm; $\zeta = 40.8 \pm 1.2$ mV (10 mM KNO_3, in dionized water). The D_h and ζ were then measured after adjusting the pH from 3.5 to between 2 and 4.5, at room temperature and after heating NA dispersions to 65°C (fig. 6 and tabulated in table S2, supporting information.)

For unheated NA dispersions D_h remains essentially constant across all pH values studied. Conversely, after adjusting pH and heating, D_h either contracts with reducing pH or swells with increasing pH (from pH 3.5). Significantly, D_h of NAs post-heating is consistent with the size formed directly from heating the initial copolymer latex, at any respective pH value. This trend underscores the significance of the thermoresponsive nature of the copolymer, with temperature being able to trigger changes in size for not only the copolymer latex, but also for the NAs. Zeta (or electrokinetic) potential is a measure of the potential difference in the interfacial double layer at the slip plane. So it is the effective surface charge (not total

charge) of the aggregates that is being measured. For unheated samples ζ remains constant when the pH is taken below 3.5. This is consistent with the proposal that amino groups located at the surfaces are entirely protonated, as pH $\ll$ pK_a. As pH is taken above 3.5 the ζ decreases quite rapidly as amino groups are presumably deprotonated and surfactant is able to readsorb at the particle-aqueous interface with increasing pH. Readsorbing surfactant might actually contribute to the loss of (positive) surface charge, as represented by a decrease in ζ. Regardless, the surfactant is unable to compensate for the loss of charge-stability as pH is taken above 4.5, given that the aggregates phase separate irreversibly.

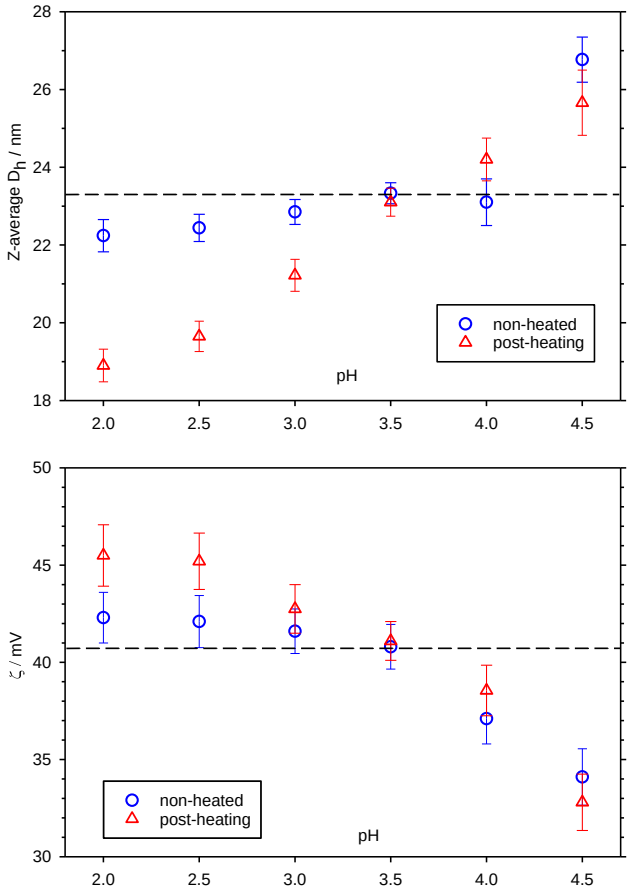

Figure 6: (Upper) Z-average hydrodynamic diameter (D_h) of self-assembled aggregates (formed at pH 3.5) as a function of pH. (Lower) Zeta potential (ζ) of self-assembled aggregates (formed at pH 3.5) as a function of pH. In both plots, the samples with the pH adjusted at room temperature are blue hollow circles and aggregates formed post-heating are red hollow triangles. The dashed lines represent the respective D_h or ζ of the aggregate at pH 3.5 and are guides for the eye. Error bars are the standard deviations of all data collected, from a minimum of three replicates (DLS) or 5 replicates (electrophoresis).

When the same aggregates are heated and returned to room temperature, ζ increases for NAs with their pH adjusted below pH 3.5. Interestingly, this suggests that temperature facilitates the release of latent charge located in the interior of the copolymer aggregates. Despite the lumpy structure of the copolymer, there are still DMAEMA units incorporated randomly in polymer chains and a distribution of some polymer chains richer or poorer in DMAEMA. Similarly to the formation of NAs from the copolymer latex, a high polymer concentration ($\geq$10% w/w) is required in order to see a compaction of the particle size (and a further redistribution of charged DMAEMA groups to the surface) as pH is reduced. This implies that breaking-up the physical polymer network at elevated temperature, forces re-assembly of polymer chains and alters the distribution of DMAEMA groups at the aggregate surfaces (i.e. in the corona).

Zeta potential values are particularity useful for giving insight into long-term stability of colloidal systems. Bearing in mind that the chemical environment (pH, concentration, ionic strength, additives etc.) markedly impacts Zeta potential. In the absence of effective stabilisation by surfactants, the magnitude of $\zeta \geq$40 mV, suggests that the positively charged aggregates are very stable over the acidic pH regime (and mild ionic strength).

Interfacial and assembly properties

Like their low-molecular weight surfactant counterparts, polymers can modify properties of liquid surfaces, if they possess sufficient amphiphilic character. It is the same amphilicity that drives the microphase separation of hydrophilic and hydrophobic segments in order to minimise hydrophobic-water interactions.[52] Pyrene was used as a fluorescent probe to provide direct evidence of the existence of hydrophobic microdomains. Surface tension measurements were carried out over the same concentration range (fig. 7.) Polymer dispersions were dialysed in order to isolate the copolymers from any residual surfactant. Data were collected at pH 3.5 only. Although pH should impact the critical assembly concentration (CAC) and surface activity of the copolymer, the purpose is to highlight the general concentration-dependant

assembly properties of this copolymer system, rather than explore trends across pH.

Fluorescence probe experiments are convenient to assess the CAC of copolymers.[53,54] Pyrene is a frequently used probe, since the ratio in the intensity (I) of the first (λ=373 nm) and third (λ=383 nm) vibration bands in emission spectra, is indicative of the chromophore environment polarity (fig. S4, supporting information). By keeping the pyrene concentration fixed and varying the copolymer concentration, I_{373}/I_{383} can be plotted to determine the CAC. From fig.7, it can be seen that at low copolymer concentration, I_{373}/I_{383} is constant, indicating that the pyrene is sensing mainly an aqueous environment, consistent with the copolymer existing as non-aggregated, free-polymer. At $\sim$ 0.7 mg mL, there is a sharp decrease in I_{373}/I_{383}. Here, the pyrene is reporting from hydrophobic microenvironments of the aggregates; this sharp change in environment polarity identifies the CAC, = 0.72 mg mL^{-1}.

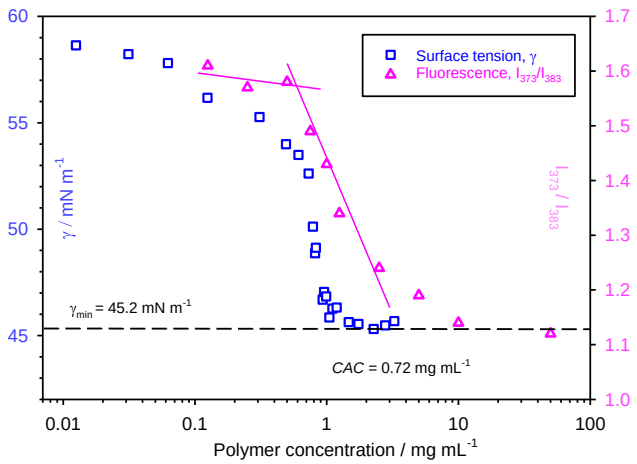

Figure 7: Surface activity (Blue squares, left axis) and the ratio of the intensity (I) of the 1st (373 nm) and 3rd (383 nm) vibration bands, from the fluorescence excitation spectra of pyrene (pink triangles, right axis), both as a function of copolymer concentration, at pH 3.5.

From the surface tension-concentration curve it is clear that the copolymer exhibits reasonable surface activity, with a minimum surface tension (γ_{min}) = 45.2 mN m^{-1}. Up until $\sim$ 0.6 mg mL^{-1} surface tension decreases gradually, before falling sharply to γ_{min}, representing the saturation of the liquid-air surface. The concentration for γ_{min} and a CAC is in good agreement with the fluorescence results also seen in fig.7. A noticeable surface activ-

ity, together with the formation of NAs may be linked to the lumpy microstructure of the copolymer.

Given the ability of this polymer to modify the air-liquid interface, it can be defined as a 'polymeric surfactant'. This is a useful definition since it is clearly distinguishable from a 'polysoap' (which is an amphiphilic random copolymer which contains a surface-active component in it polymer repeat unit and so assembles intramolecularly[55]) and is perhaps more subtly distinct from classic block copolymers (which have clearly segregated blocks and have much lower chemical composition distributions.) In table 1, the interfacial and assembly properties are compared with related amphiphilic copolymers from the literature. It must be recognised that these solution and interfacial properties depend on the chemical nature of monomers, polymer composition/architecture and molecular weight amongst other parameters. Therefore, the purpose of table 1 is to highlight the broad similarity in behaviour, in spite of the differences between polymer systems. The limited water solubility of many amphiphilic copolymers restricts interfacial studies in aqueous solution to more hydrophilic copolymers which can be directly dissolved in solution. Importantly, this random cationic copolymer shares many properties with block copolymers, despite possessing a more ill-defined chemical architecture (and a comparably straightforward synthetic route to aqueous dispersed copolymer.) Nevertheless, the interfacial performance of this copolymer system is very much a consequence of a particular synthetic strategy (and monomer combination). As such, structure-performance relationships in less well-defined copolymers (as is the case here) probably need to be assessed on a case-by-case basis. Perhaps it is more generally true for random copolymers that without comprehensive and systematic studies then universal 'design-rules' that unify structure with specific properties (and/or performance) may prove elusive.

Table 1: Properties of comparable polymer systems. [a] D_h at pH = 3.5. [b] poly(methacryloxyethyl trimethyl ammonium chloride-co-butyl acrylateacrylamide.[56] [c] Two breaks are observed in the surface tension plot, which are referred to as the first (0.7 mg mL^{-1}) and second (0.4 mg mL^{-1}) CAC, respectively. [d] poly(methyl methacrylate-co-2-dimethylaminoethyl methacrylate)(79 mol % DMAEMA,) at pH = 9.5.[57] [e] poly(butyl acrylate-b-3-acrylamidopropyltrimethylammonium chloride).[58] [f] poly(allyl alcohol 1,2-butoxylate-b-ethoxylate), commercially available from Aldrich.[58]

System	$CAC/(mg\,mL^{-1})$	$\gamma_{min}/(mN\,m^{-1})$	D_h/nm
random			
poly(DMAEMA-co-MMA) $-$*this study*	0.7	45	23 [a]
poly(MTAC-co-BAAM) [b]	0.07-0.4 [c]	47	*not reported*
block			
poly(DMAEMA-b-MMA) [d]	0.5	46	10-27
poly(BA_{81}-b-$AMPTMA_{55}$) [e]	*not reported*	50	54
poly(BO_{37}-b-EO_{100}) [f]	0.2	32	15

NA morphology and aggregation properties

Earlier, DLS was used to study the relative size of NAs, without providing detailed internal stuctural information. This is because only an effective diameter can be delineated from DLS. On the other hand, small-angle neutron scattering (SANS) is a useful technique for determining the time-average shape of particles over the colloidal length-scale.[59] In addition to size and shape information (contained within the particle form factor, P(Q)), M_w of aggregates can be approximated, allowing for the weight-average aggregation number of the self-assembled NAs to be estimated.

In fig. 8 the SANS profiles for the copolymer latex, post-heating are given, along with fits to the single particle P(Q). At pH 5, the copolymer latex does not undergo a transition to NAs. As such, particles can be seen to scatter to lower-Q (i.e. lower angle) with a higher absolute intensity (since intensity scales with the particle volume squared) in comparison to the smaller NAs. Although not shown in the main text, (fig. S5, supporting information), the copolymer latex can be fit to a spherical P(Q) across all pH values. In fact, this is reassuring that DLS gives an acceptable approximation of the size of the larger copolymer

latex.

The NAs, however, could not be well fit to a spherical P(Q). 'Goodness' of fits was ensured by fixing known parameters (e.g. Φ) and floating unknown parameters to minimise the reduced χ^2. A good first approximation of the morphology of a particle is given by the power law of the Q decay, over an intermediate Q-range.[59] Spherical particle decay $\propto Q^{-4}$, whereas ellipsoids decay $\propto Q^{-3}$, with 2D disks/sheets decaying $\propto Q^{-2}$. The mid-Q scattering decay for the NAs is $\propto Q^{-3}$, implying that particles may be more elongated in shape. Indeed, it was found that particle morphology could be best fit to an oblate ellipsoidal form factor (see supporting information). Fitting the data by applying sensible constraints (from sample preparation, i.e Φ, ρ_p and ρ_s and from size parameters extracted from Guinier plots (fig. S6, supporting information) and DLS,) the data could not be well represented as either polydisperse spheres or prolate ellipsoids. Here the shape of the particles can be described by a polar, r_a and equatorial, r_b axis, where $r_a < r_b$, and r_b/r_a is defined as the aspect ratio. The fit parameters for the NAs across different pH values are given in table 2.

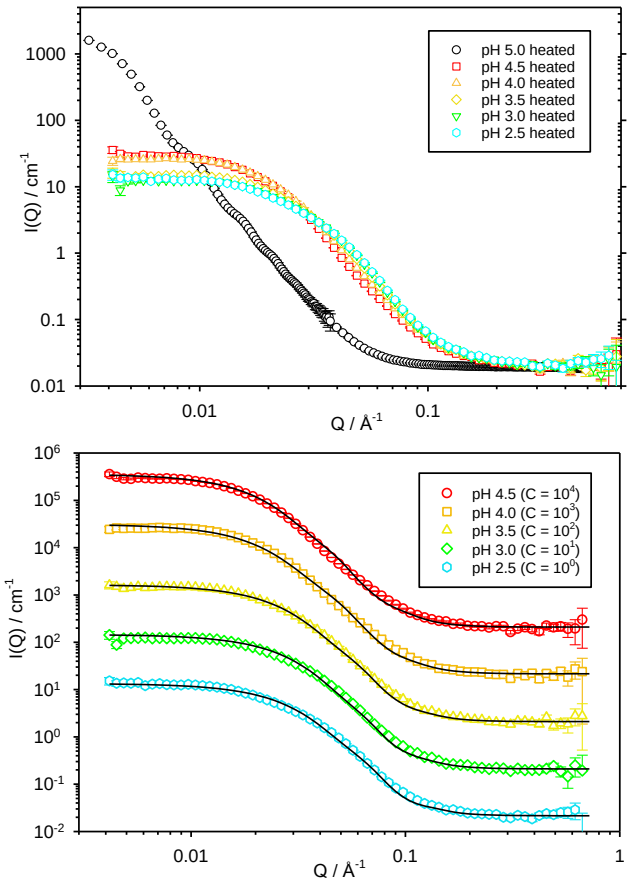

Figure 8: (Upper) SANS profiles of copolymer latex after heating, as a function of pH. (Lower) SANS profiles off-set for clarity, the multiplier, C is given in the legend. The black line, in each case, is the fit to the particle form factor (P(Q)).

Table 2: Ellipsoidal P(Q) fit parameters. The dashed line represents the pH threshold for forming self-assembled nano-aggregates. At pH 5 the copolymer latex was fit to a spherical P(Q), so that $r_a = r_b$ for an equivalent 'ellipsoid'. Self-assembled aggregates formed at all other pH values were fit to the oblate ellipsoid P(Q), where $r_a < r_b$. Representative errors in r_a and r_b are ± 0.2 nm.

Ellipsoid fit parameters				
pH	r_a/nm	r_b/nm	(r_b/r_a)	N_{agg}
5.0	58.30	$r_a = r_b$	1.0	n/a
4.5	4.18	13.97	3.4	72
4.0	4.16	13.00	3.1	65
3.5	3.82	10.02	2.6	40
3.0	3.80	9.51	2.5	35
2.5	3.71	9.30	2.5	34

SANS fits reveal that the decrease in size (as also observed by DLS) is mainly due to a reduction in the major r_b axis, manifesting as a reduction in the aspect ratio. From pH 4.5 to pH 2.5, the aspect ratio decreases from 3.4 to 2.5, i.e particles are becoming more compact/spherical. Zeta- potential measurements already provided a connect between increasing surface potential of the NAs, as pH is reduced (and the copolymer chains are dispersed by temperature). Further evidence of the increased charging of the NAs at lower pH can also be appreciated through the inter-particle S(Q), which is observable even at low copolymer concentration, when the copolymers are measured with no background electrolyte (fig. 9.) A much larger depression in low-Q scattering is evident in the profile of the NAs at pH 2.5 relative to the profile from NAs at pH 4.5 (which can be fit at dilute concentration to a single particle P(Q)), i.e the inter-particle interference effects are more pronounced due to screened coulomb repulsion between more strongly charged particles. An adequate fit at pH 2.5 can only be achieved by inclusion of a charged structure factor in addition to the single particle P(Q), and this is accounted for in this work by a Hayter mean square approximation (for more detail see supporting information.)

On first principle, compaction of particles as pH is lowered can be crudely understood with reference to the so called *critical packing parameter*,[60] used to predict the preferred aggregate structure adopted by amphiphiles. This commonly used approach anticipates that increasing the size of the amphiphle 'headgroup' (or the corona for copolymers) would lead to an increase in aggregate curvature (assuming the tail structure of the amphiphile remains the same). An increase in density of positive charge at the surface, as pH is reduced, should increase the like-charge electrostatic repulsion between adjacent DMAEMA-rich chains, increasing the effective size of the corona chains located at the interface. Typically with block copolymers, however, the morphology of polymer micelles is usually governed by the swelling/deswelling of the corona, even when the degree of polymeristaion of the corona forming monomer is low.[51,61] For well defined block copolymers, increasingly charging the corona forming monomers, causes polymer chains to extend into the aqueous solvent, behav-

ing like an osmotic brush.[51] Reducing the charge of the corona forming monomer by tuning pH or ionic strength leads to a contraction of the corona.

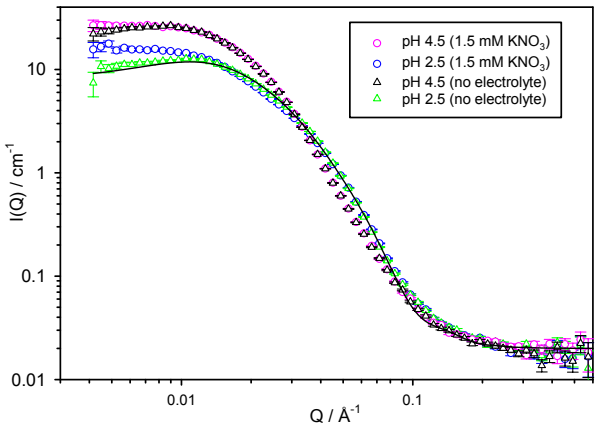

Figure 9: SANS profiles of copolymer nano-aggregates at pH 4.5 and pH 2.5, both in the presence of electrolyte and with no electrolyte to screen electrostatic inter-particle interactions. The solid black line is the fit to the nano-aggregate at pH 2.5 with no electrolyte. The fit includes a charged structure factor S(Q) in addition to an ellipsoidal form factor to fit the low-Q data.

In this case the low degree of polymerisation of DMAEMA in the copolymer structure is important, together with the lumpy (and not block structure) and the broad Đ of the copolymer. Eisenberg et al. estimated corona layers to be less that 0.3 nm in thickness in poly(styrene-b-acrylic acid) copolymers with similarly low contents of corona forming monomer.[62] The lumpy incorporation of DMAEMA, i.e some MMA groups may interrupt consecutive sequences of DMAEMA units, reducing the propensity to extend into solution. Chains richer in DMAEMA could be more likely to straddle the interface, rather than extend into solution. It is not unreasonable to assume the predominant result of a higher concentration of interfacial charge of the NAs results in a compaction of the aggregates since the degree of polymerisation of DMAEMA is low, along with incomplete segregation of the two monomers. In any case, NAs cannot be merely conceptualised as classic polymer micelles. With reducing pH, aggregation number N_{agg} of the aggregates falls by more than a factor of 2, from 72 to 35. This is consistent with an increase in the amphiphile solubility as more

DMAEMA groups are protonated.

One final point to note is that the SANS profiles of the NAs are absent of any high-Q scattering features, indicative of core-shell form factors. This is probably the result of two factors. Firstly, there is limited neutron-contrast between what should be a DMAEMA-rich corona and DMAEMA-poor core, given the similar chemical structures of MMA and DMAEMA. Secondly the DMAEMA-rich region would be expected to be very thin (less than 0.3 nm) compared to the size of the aggregates. Future experiments using deuterated MMA (or DMAEMA) could provide enough contrast to extract information on the composition (and thickness) of any DMAEMA-rich region stabilising the NAs.

Conclusion

A copolymer, poly(methyl methacrylate-co-2-dimethylaminoethyl methacrylate) (poly(MMA-co-DMAEMA)), with a low mole fraction of DMAEMA ($\sim 10\%$) was prepared by a routine emulsion polymerisation. DMAEMA was incorporated in a 'lumpy' (or 'blocky' but not block) fashion which allowed the hydrophilicity of the copolymer to be tuned by adjusting the pH and temperature. Nanoscale-aggregates were formed in aqueous solution directly from the surfactant-stabilised latex by pH and temperature triggers.

The copolymer system presented in this paper is significant for two distinct reasons: **(1)** at the beginning of this article the following question was posed: "could a random copolymer with a lumpy arrangement of its monomers stabilise interfaces and micellar-like aggregates?" The main physiochemical properties of the 'general' copolymer system (properties broadly shared by the free-polymer at all pH values < 5) and the pH-property dependent nano-aggregates (NAs) are summarised in table 3. It can be concluded that despite possessing a more ill-defined chemical structure, this random lumpy copolymer displays many properties (surface-activity at the air-water interface and a defined critical association concentration (CAC)) expected of more well-defined block copolymers (table 1). However, the broad Đ and

lumpy incorporation of DMAEMA seem to be reasons for the aggregation behaviour, which cannot be simply conceptualised as aggregating like classic polymer micelles. In addition, it is the effective surface charge density of DMAEMA which plays a key role in governing the aggregate morphology.

Table 3: Overview of the general properties of poly(MMA-co-DMAEMA) and pH-dependent aggregate properties. [a] Dispersity (gel-permeation chromatography). [b] Surface tension at the CAC (surface-tensiometry). [c] CAC (fluorescence spectroscopy). [d] Hydrodynamic diameter, (dynamic-light scattering). [e] Zeta potential, (electrophoresis). [f] Aspect ratio (r_b/r_a) and weight-average aggregation number, N_{agg} (SANS).

	$M_w/(kg\ mol^{-1})$ [a]	$Đ$ [a]	$\gamma_{min}/(mN\ m^{-1})$ [b]	$CAC/(mg\ mL^{-1})$ [c]
general	15.8	1.88	45.2	0.72
pH	D_h/nm [d]	ζ/mV [e]	(r_b/r_a) [f]	N_{agg} [f]
4.5	28.6	34.1	3.4	72
4.0	24.6	37.1	3.1	65
3.5	23.1	40.8	2.6	40
3.0	21.2	41.6	2.5	35
2.5	19.7	42.1	2.5	34

Recently random copolymers have been gaining increasing attention in the literature.[27,63,64] The clear advantage held by random copolymers over block copolymers, is their comparably straightforward (and usually cheaper) synthesis. Up to now, most of this research has been directed toward replicating the tuneability of block copolymer systems, in an attempt to match the versatility of self-assembled structures. However, in this respect, block copolymers are always likely to have the upper hand, since they exhibit predictable control over the resulting morphology of the self-assembled structure by tuning molecular parameters that are controllable in the synthesis, such as the molecular weight, the degree of polymerisation of the blocks and their chemical nature.[16,65,66] Perhaps a better focus of efforts could be directed towards rapid and efficient routes to self-assembled aggregates. **(2)** typically self-assembled aggregates in aqueous solution of random copolymers are prepared similarly to their block-copolymer counterparts, via the water-induced micellisation method.[16,27] This is neither a time/material efficient or particularly environmentally-friendly process, also requiring the

separation of a volatile organic solvent. The significance of the system presented in this work, is that self-assembled aggregates can be formed in a water-only, one-pot procedure, which is straightforward and involves no organic solvents. In fact, for many industrial/practical applications it may not be necessary to dialyse the polymer dispersion and so nanoscale aggregates could be prepared via a very direct route. With obvious constraints still limiting the widespread adoption of block copolymers for industrial applications, it remains a valuable pursuit to design heuristic systems that can be applied to industrial problems today.

Acknowledgement

JCP thanks Koninklijke DSM N.V. (DSM) for the provision of a PhD studentship. The authors thank the UK Science and Technology Facilities Council (STFC) for allocation of beamtime at ISIS and associated grants for consumables and travel. This work benefited from SasView Small Angle Scattering Analysis Software Package, originally developed by the DANSE project under NSF award DMR-0520547.

Supporting Information Available

Removal of surfactant by dialysis as monitored by equilibrium surface tension, Gel permeation chromatography trace for poly(MMA-co-DMAEMA), Zeta potential measurements of copolymer latex as function of pH at room temperature, fluorescence spectroscopy spectra, SANS profiles and fits of copolymer latex across pH range, Guinier plots, Tabulated data from fig. 5 and fig. 6, SANS fitting information and SANS fit parameters described in text.

This material is available free of charge via the Internet at `http://pubs.acs.org/`.

References

(1) Nagarajan, R. Amphiphilic surfactants and amphiphilic polymers: Principles of molecular assembly. *ACS Symposium Series* **2011**, *1070*, 1–22.

(2) Jones, M. C.; Leroux, J. C. Polymeric micelles - A new generation of colloidal drug carriers. *European Journal of Pharmaceutics and Biopharmaceutics* **1999**, *48*, 101–111.

(3) York, A. W.; Kirkland, S. E.; McCormick, C. L. Advances in the synthesis of amphiphilic block copolymers via RAFT polymerization: Stimuli-responsive drug and gene delivery. *Advanced Drug Delivery Reviews* **2008**, *60*, 1018–1036.

(4) Ganta, S.; Devalapally, H.; Shahiwala, A.; Amiji, M. A review of stimuli-responsive nanocarriers for drug and gene delivery. *Journal of Controlled Release* **2008**, *126*, 187–204.

(5) Kim, H. C.; Park, S. M.; Hinsberg, W. D.; Division, I. R. Block copolymer based nanostructures: Materials, processes, and applications to electronics. *Chemical Reviews* **2010**, *110*, 146–177.

(6) Noshay, Allen,; McGrath, J. E. *Block copolymers: overview and critical survey*; Elsevier,, 2013.

(7) Chang, Y.; McCormick, C. L. Water-soluble copolymers. 49. Effect of the distribution of the hydrophobic cationic monomer dimethyldodecyl(2-acrylamidoethyl)ammonium Bromide on the solution behavior of associating acrylamide copolymers. *Macromolecules* **1993**, *26*, 6121–6126.

(8) Daswani, P.; van Herk, A. Solubility Data of Comonomer Pairs Relevant to Aqueous-Phase Study in the Emulsion Copolymerization. *Dataset Papers in Science* **2013**, *2013*, 1–5.

(9) Lee, S. B.; Russell, A. J.; Matyjaszewski, K. ATRP synthesis of amphiphilic random, gradient, and block copolymers of 2-(dimethylamino)ethly methacrylate and n-butyl methacrylate in aqueous media. *Biomacromolecules* **2003**, *4*, 1386–1393.

(10) Hoogenboom, R.; Fijten, M. W. M.; Wijnans, S.; Van Den Berg, A. M. J.; Thijs, H. M. L.; Schubert, U. S. High-throughput synthesis and screening of a library of random and gradient copoly(2-oxazoline)s. *Journal of Combinatorial Chemistry* **2006**, *8*, 145–148.

(11) Montaudo, M. S. Determination of the compositional distribution and compositional drift in styrene/maleic anhydride copolymers. *Macromolecules* **2001**, *34*, 2792–2797.

(12) Mühlebach, a.; Gaynor, S. G.; Matyjaszewski, K. Synthesis of amphiphilic block copolymers by atom transfer radical polymerization (ATRP). *Macromolecules* **1998**, *31*, 6046–6052.

(13) Chong, B. Y. K.; Le, T. P. T.; Moad, G.; Rizzardo, E.; Thang, S. H. More versatile route to block copolymers and other polymers of complex architecture by living radical polymerization: the RAFT process. *Macromolecules* **1999**, *32*, 2071–2074.

(14) Barner, L.; Davis, T. P.; Stenzel, M. H.; Barner-Kowollik, C. Complex macromolecular architectures by reversible addition fragmentation chain transfer chemistry: Theory and practice. *Macromolecular Rapid Communications* **2007**, *28*, 539–559.

(15) Keddie, D. J. A guide to the synthesis of block copolymers using reversible-addition fragmentation chain transfer (RAFT) polymerization. *Chem. Soc. Rev.* **2014**, *43*, 496–505.

(16) Mai, Y.; Eisenberg, A. Self-assembly of block copolymers. *Chemical Society Reviews* **2012**, *41*, 5969.

(17) Rösler, A.; Vandermeulen, G. W. M.; Klok, H. A. Advanced drug delivery devices via self-assembly of amphiphilic block copolymers. *Advanced Drug Delivery Reviews* **2012**, *64*, 270–279.

(18) Ilhan, F.; Galow, T. H.; Gray, M.; Clavier, G.; Rotello, V. M. Giant vesicle formation through self-assembly of complementary random copolymers [10]. *Journal of the American Chemical Society* **2000**, *122*, 5895–5896.

(19) Liu, X.; Kim, J.-S.; Wu, J.; Eisenberg, A. Bowl-Shaped Aggregates from the Self-Assembly of an Amphiphilic Random Copolymer of Poly(styrene- co -methacrylic acid). *Macromolecules* **2005**, *38*, 6749–6751.

(20) Burd, C.; Week, M. Self-sorting in polymers. *Macromolecules* **2005**, *38*, 7225–7230.

(21) Guo, P.; Guan, W.; Liang, L.; Yao, P. Self-assembly of pH-sensitive random copolymers: Poly(styrene-co-4-vinylpyridine). *Journal of Colloid and Interface Science* **2008**, *323*, 229–234.

(22) Deng, Y.; Li, Y.; Wang, X. Colloidal sphere formation, H-aggregation, and photoresponsive properties of an amphiphilic random copolymer bearing branched Azo side chains. *Macromolecules* **2006**, *39*, 6590–6598.

(23) Tian, F.; Yu, Y.; Wang, C.; Yang, S. Consecutive morphological transitions in nanoaggregates assembled from amphiphilic random copolymer via water-driven micellization and light-triggered dissociation. *Macromolecules* **2008**, *41*, 3585–3588.

(24) Sun, G.; Zhang, M.; He, J.; Ni, P. Synthesis of amphiphilic cationic copolymers poly[2-(methacryloyloxy)ethyl trimethylammonium chloride-co-stearyl methacrylate] and their self-assembly behavior in water and water-ethanol mixtures. *Journal of Polymer Science, Part A: Polymer Chemistry* **2009**, *47*, 4670–4684.

(25) Wu, X.; Qiao, Y.; Yang, H.; Wang, J. Self-assembly of a series of random copolymers bearing amphiphilic side chains. *Journal of Colloid and Interface Science* **2010**, *349*, 560–564.

(26) Dan, K.; Bose, N.; Ghosh, S. Vesicular assembly and thermo-responsive vesicle-to-micelle transition from an amphiphilic random copolymer. *Chemical Communications* **2011**, *47*, 12491.

(27) Li, L.; Raghupathi, K.; Song, C.; Prasad, P.; Thayumanavan, S. Self-assembly of random copolymers. *Chemical communications (Cambridge, England)* **2014**, *50*, 13417–32.

(28) Hirai, Y.; Terashima, T.; Takenaka, M.; Sawamoto, M. Precision Self-Assembly of Amphiphilic Random Copolymers into Uniform and Self-Sorting Nanocompartments in Water. *Macromolecules* **2016**, acs.macromol.6b01085.

(29) Demirel, G. B.; Von Klitzing, R. A new multiresponsive drug delivery system using smart nanogels. *ChemPhysChem* **2013**, *14*, 2833–2840.

(30) Wang, F. P.; Zhang, J. Y.; Mu, H. P.; Li, W. X.; Yuan, T.; Du, X. Z. Preparation and application in drug controlled delivery of pH-sensitive P(CE- co -DMAEMA- co -MEG) hydrogel. *Journal of Applied Polymer Science* **2014**, *131*, n/a–n/a.

(31) Mostafa, K. M.; Samarkandy, A. R.; El-Sanabary, A. A. Preparation of poly (DMAEM)-cross linked pregelled starch graft copolymer and its application in waste water treatments. *Carbohydrate Polymers* **2011**, *86*, 491–498.

(32) Han, D.; Boissiere, O.; Kumar, S.; Tong, X.; Tremblay, L.; Zhao, Y. Two-Way CO 2 -Switchable Triblock Copolymer Hydrogels. *Macromolecules* **2012**, *45*, 7440–7445.

(33) Siu, M. H.; He, C.; Wu, C. Formation of mesoglobular phase of amphiphilic copolymer chains in dilute solution: Effect of comonomer distribution. *Macromolecules* **2003**, *36*, 6588–6592.

(34) Kujawa, P.; Tanaka, F.; Winnik, F. M. Temperature-dependent properties of telechelic hydrophobically modified poly(N-isopropylacrylamides) in water: Evidence from light scattering and fluorescence spectroscopy for the formation of stable mesoglobules at elevated temperatures. *Macromolecules* **2006**, *39*, 3048–3055.

(35) Aseyev, V.; Hietala, S.; Laukkanen, A.; Nuopponen, M.; Confortini, O.; Du Prez, F. E.; Tenhu, H. Mesoglobules of thermoresponsive polymers in dilute aqueous solutions above the LCST. *Polymer* **2005**, *46*, 7118–7131.

(36) Hunter, R. J. Recent developments in the electroacoustic characterisation of colloidal suspensions and emulsions. *Colloids and Surfaces A: Physicochemical and Engineering Aspects* **1998**, *141*, 37–65.

(37) Arnold, O. et al. Mantid - Data analysis and visualization package for neutron scattering and μ SR experiments. *Nuclear Instruments and Methods in Physics Research, Section A: Accelerators, Spectrometers, Detectors and Associated Equipment* **2014**, *764*, 156–166.

(38) Wignall, G. D.; Bates, F. S. Absolute calibration of small-angle neutron scattering data. *Journal of Applied Crystallography* **1987**, *20*, 28–40.

(39) Sasview for small angle scattering analysis. `http://www.sasview.org/`.

(40) Maxwell, I. a.; Maxwell, I.; Morrison, B. R.; Napper, D. H.; Morrison, B.; Napper, D.; Gilbert, R. G.; Gilbert, R. Entry of free radicals into latex particles in emulsion polymerization. *Macromolecules* **1991**, *24*, 1629–1640.

(41) Van Doremaele, G. H. J.; Van Herk, A. M.; German, A. L. Modelling of emulsion copolymer microstructure. *Polymer International* **1992**, *27*, 95–108.

(42) Wang, S. T.; Poehlein, G. W. Studies of water-soluble oligomers formed in emulsion copolymerization. *Journal of Applied Polymer Science* **1994**, *51*, 593–604.

(43) Wang, S. T.; Poehlein, G. W. Characterization of water-soluble oligomer in acrylic acid-styrene emulsion copolymerization. *Journal of Applied Polymer Science* **1993**, *50*, 2173–2183.

(44) van de Wetering, P.; Zuidam, N. J.; van Steenbergen, M. J.; van der Houwen, O. A. G. J.; Underberg, W. J. M.; Hennink, W. E. A mechanistic study of the hydrolytic stability of poly (2-(dimethylamino) ethyl methacrylate). *Macromolecules* **1998**, *31*, 8063–8068.

(45) Scheerder, J.; Langermans, H. The synthesis, interfacial, and colloidal properties of waterborne cationic methacrylic co-polymers. *Colloid and Polymer Science* **2014**, *292*, 991–1001.

(46) Qiu, J.; Charleux, B.; Matyjaszewski, K.; Pierre, Â.; Curie, M. Controlled / living radical polymerization in aqueous media : homogeneous and heterogeneous systems. *Progress in Polymer Science* **2001**, *26*, 2083–2134.

(47) Cotanda, P.; Wright, D. B.; Tyler, M.; O'Reilly, R. K. A comparative study of the stimuli-responsive properties of DMAEA and DMAEMA containing polymers. *Journal of Polymer Science, Part A: Polymer Chemistry* **2013**, *51*, 3333–3338.

(48) Heyda, J.; Soll, S.; Yuan, J.; Dzubiella, J. Thermodynamic description of the LCST of charged thermoresponsive copolymers. *Macromolecules* **2014**, *47*, 2096–2102.

(49) De Souza, J. C. P.; Naves, A. F.; Florenzano, F. H. Specific thermoresponsiveness of PMMA-block-PDMAEMA to selected ions and other factors in aqueous solution. *Colloid and Polymer Science* **2012**, *290*, 1285–1291.

(50) Liu, S.; Weaver, J. V. M.; Tang, Y.; Billingham, N. C.; Armes, S. P.; Tribe, K. Synthesis of shell cross-linked micelles with pH-responsive cores using ABC triblock copolymers. *Macromolecules* **2002**, *35*, 6121–6131.

(51) Laaser, J. E.; Jiang, Y.; Sprouse, D.; Reineke, T. M.; Lodge, T. P. pH- and ionic-strength-induced contraction of polybasic micelles in buffered aqueous solutions. *Macromolecules* **2015**, *48*, 2677–2685.

(52) Raffa, P.; Wever, D. A. Z.; Picchioni, F.; Broekhuis, A. A. Polymeric surfactants: Synthesis, properties, and links to applications. *Chemical Reviews* **2015**, *115*, 8504–8563.

(53) Zhao, C.-l.; Winnik, M. a.; Croucher, M. D. Fluorescence Probe Techniques Used To Study Micelle Formation in Water-Soluble Block Copolymers. *Langmuir* **1990**, *6*, 514–516.

(54) Topel, Ö.; ÇakÄśr, B. A.; Budama, L.; Hoda, N. Determination of critical micelle concentration of polybutadiene-block-poly(ethyleneoxide) diblock copolymer by fluorescence spectroscopy and dynamic light scattering. *Journal of Molecular Liquids* **2013**, *177*, 40–43.

(55) Laschewsky, A. Molecular concepts, self-organisation and properties of polysoaps. **1995**, 1–86.

(56) Cao, X.; Tan, Y.; Xu, G.; Wu, D. Aggregation Behavior of Cationic Copolymer Methacryloxyethyl Trimethyl Ammonium ChlorideâĂŘButyl AcrylateâĂŘAcrylamide in Aqueous Solution. *Journal of Dispersion Science and Technology* **2008**, *29*, 70–76.

(57) Baines, F. L.; Billingham, N. C.; Armes, S. P. Synthesis and Solution Properties of Water-Soluble Hydrophilic-Hydrophobic Block Copolymers. *Macromolecules* **1996**, *29*, 3416–3420.

(58) Garnier, S.; Laschewsky, A. New amphiphilic diblock copolymers: Surfactant properties and solubilization in their micelles. *Langmuir* **2006**, *22*, 4044–4053.

(59) Hollamby, M. J. Practical applications of small-angle neutron scattering. *Physical Chemistry Chemical Physics* **2013**, *15*, 10566–10579.

(60) Israelachvili, J. N.; Mitchell, D. J.; Ninham, B. W. Theory of self-assembly of hydrocarbon amphiphiles into micelles and bilayers. *Journal of the Chemical Society, Faraday Transactions 2* **1976**, *72*, 1525.

(61) Dai, S.; Ravi, P.; Tam, K. C. pH-Responsive polymers: synthesis, properties and applications. *Soft Matter* **2008**, *4*, 435.

(62) Zhang, L.; Eisenberg, a. Multiple morphologies and characteristics of 'crew-cut' micelle-like aggregates of polystyrene-b-poly(acrylic acid) diblock copolymers in aqueous solutions. 1996.

(63) Wang, D.; Wang, X. Amphiphilic azo polymers: Molecular engineering, self-assembly and photoresponsive properties. *Progress in Polymer Science* **2013**, *38*, 271–301.

(64) Zhao, Y.; Sakai, F.; Su, L.; Liu, Y.; Wei, K.; Chen, G.; Jiang, M. Progressive macromolecular self-assembly: From biomimetic chemistry to bio-inspired materials. *Advanced Materials* **2013**, *25*, 5215–5256.

(65) Riess, G. Micellization of block copolymers. *Progress in Polymer Science (Oxford)* **2003**, *28*, 1107–1170.

(66) Srinivas, G.; Discher, D. E.; Klein, M. L. Self-assembly and properties of diblock copolymers by coarse-grain molecular dynamics. *Nature materials* **2004**, *3*, 638–644.

Graphical TOC Entry